

1

2

3

4 The Mimivirus L375 Nudix enzyme hydrolyzes the 5' mRNA cap

5 Short title: Mimivirus L375 mRNA decapping enzyme

6

7

8 Grace Kago^{1#a} and Susan Parrish^{1*}

9

10

11

12

13

14 ¹Department of Biology, McDaniel College, Westminster, Maryland, United States of

15 America

16

17 ^{#a}Current Address: Department of Molecular Biosciences, Institute for Cellular and

18 Molecular Biology, The University of Texas at Austin, Austin, Texas, United States of

19 America

20

21

22 *Corresponding author

23 E-mail: sparrish@mcdaniel.edu (SP)

24 **Abstract**

25 The giant Mimivirus is a member of the nucleocytoplasmic large DNA viruses
26 (NCLDV), a group of diverse viruses that contain double-stranded DNA (dsDNA)
27 genomes that replicate primarily in eukaryotic hosts. Two members of the NCLDV,
28 Vaccinia Virus (VACV) and African Swine Fever Virus (ASFV), both synthesize Nudix
29 enzymes that have been shown to decap mRNA, a process thought to accelerate viral and
30 host mRNA turnover and promote the shutoff of host protein synthesis. Mimivirus
31 encodes two Nudix enzymes in its genome, denoted as L375 and L534. Importantly,
32 L375 exhibits sequence similarity to ASFV-DP and eukaryotic Dcp2, two Nudix
33 enzymes shown to possess mRNA decapping activity. In this work, we demonstrate that
34 recombinant Mimivirus L375 cleaves the 5' m⁷GpppN mRNA cap, releasing m⁷GDP as a
35 product. L375 did not significantly cleave mRNAs containing an unmethylated 5'GpppN
36 cap, indicating that this enzyme specifically hydrolyzes methylated-capped transcripts. A
37 point mutation in the L375 Nudix motif completely eliminated cap hydrolysis, showing
38 that decapping activity is dependent on this motif. Addition of methylated cap derivatives
39 or uncapped RNA inhibited L375 decapping activity, suggesting that L375 recognizes its
40 substrate through interaction with both the mRNA cap and RNA body.

41

42 **Introduction**

43 The giant Mimivirus, which infects *Acanthamoeba* species, possesses a 1.2 Mb
44 genome encoding over 900 proteins [1-3]. Interestingly, Mimivirus rivals some small

45 bacterial species with respect to physical and genome size, and was the first virus
46 identified to encode some of its own translational components [1-3]. Mimivirus is a
47 member of the nucleocytoplasmic large DNA viruses (NCLDV), a group that currently
48 includes seven viral families: *Poxviridae*, *Asfarviridae*, *Iridoviridae*, *Phycodnaviridae*,
49 *Mimiviridae*, *Ascoviridae*, and *Marseilleviridae* [4-8]. While many members of the
50 NCLDV share a subset of conserved genes, the evolutionary origins and relationships of
51 the NCLDV remain controversial [4-7, 9].

52 The Nudix hydrolase motif is a conserved amino acid sequence found in a diverse
53 group of enzymes that typically cleave *nucleoside diphosphates* linked to another moiety
54 *X* [10]. Nudix enzymes are nearly universal, found in prokaryotes, eukaryotes, and some
55 viruses [4, 5, 11, 12]. Two NCLDV families, *Poxviridae* and *Asfarviridae*, encode Nudix
56 enzymes that possess intrinsic mRNA decapping activity, a process that leads to mRNA
57 degradation and subsequent inhibition of gene expression [13-15].

58 The prototypic poxvirus, Vaccinia Virus (VACV), encodes two Nudix enzymes in
59 its genome termed D9 and D10. The D9R (VACV-WR_114) and D10R (VACV-
60 WR_115) genes lie adjacent to each other in the genome and encode proteins that share
61 ~20% amino acid identity but are expressed at different times during infection [16-18].
62 Prior genetic studies showed that over-expression of either D9R or D10R resulted in
63 accelerated turnover of mRNAs containing 5' m⁷GpppN caps, a structural feature of both
64 VACV and eukaryotic host mRNAs [17]. While deletion of D9R did not cause any
65 obvious defects, deletion or inactivation of D10R resulted in persistence of viral and host
66 mRNAs and a delay in the shutoff of host protein synthesis [17-19]. Subsequent
67 biochemical experiments confirmed that both D9 and D10 cleave the mRNA cap,

68 releasing m⁷GDP as a product [13, 14]. Together, these data suggest that VACV D9 and
69 D10 decap viral and host mRNAs to facilitate mRNA turnover and the shutoff of host
70 protein synthesis, thereby promoting viral infection.

71 The sole member of *Asfarviridae*, African Swine Fever Virus (ASFV), contains a
72 gene (termed g5R in strain Malawi and D250 in strain Ba71V) that encodes the Nudix
73 enzyme denoted as ASFV-DP [20, 21]. Although ASFV-DP does not share significant
74 sequence similarity to VACV D9 or D10, it does exhibit sequence similarity to Dcp2, an
75 mRNA decapping enzyme found in yeasts and mammals, along with other multicellular
76 eukaryotes [12, 21-26]. ASFV-DP was shown to cleave a broad range of substrates,
77 including diphosphoinositol polyphosphates, GTP, and the 5' m⁷GpppN cap when
78 attached to an RNA moiety [15, 20]. Subsequent *in vivo* studies revealed that over-
79 expression of ASFV-DP increases viral and host mRNA turnover, supporting the idea
80 that ASFV-DP mediates mRNA decapping and destabilization during infection [21]

81 The Mimivirus genome encodes two putative Nudix enzymes in its genome,
82 termed L375 (NCBI ID: YP_003986880) and L534 (NCBI ID: YP_003987047). Of the
83 characterized viral Nudix enzymes, L375 is most similar to the ASFV-DP mRNA
84 decapping enzyme, sharing ~21% amino acid identity. In contrast, L534 does not exhibit
85 significant similarity to any of the known viral or eukaryotic mRNA decapping enzymes,
86 instead showing sequence similarity to uncharacterized Nudix enzymes of other giant
87 viruses, bacteria, and single-celled eukaryotes. Given the sequence similarity between
88 L375 and ASFV-DP, we chose to focus this work exclusively on Mimivirus L375.

89 To determine if Mimivirus L375 can cleave the mRNA cap, a recombinant
90 version of this protein was expressed in bacteria and purified by affinity chromatography.

91 Recombinant L375 cleaved the 5' m⁷GpppN mRNA cap, releasing m⁷GDP as a product,
92 a reaction dependent on an intact Nudix motif. Importantly, L375 did not significantly
93 cleave unmethylated GpppG capped mRNAs, suggesting that L375 specifically
94 recognizes the methylated mRNA cap structure. Addition of uncapped RNA to the
95 reaction significantly inhibited L375 cap cleavage activity. Furthermore, L375 decapping
96 activity was reduced in the presence of certain methylated cap derivatives, suggesting
97 that L375 uses both the RNA and cap moieties to locate target substrates.

98

99 **Materials and methods**

100 **Plasmid design**

101 Mimivirus L375 appended with a C-terminal 10X histidine tag was generated by
102 GeneArt (Life Technologies) for codon-optimized expression in *Escherichia coli*. The
103 synthetic L375 gene was then amplified by the polymerase chain reaction (PCR) using
104 the oligonucleotide primers: 5'-ATG GAA TAT GAA ACC AAC TTT CGC AAA AAA
105 CAC ATT TG and 5'-GCG CGC AAG CTT TTA GTG ATG ATG GTG GTG ATG
106 GTG ATG ATG ATG. The resulting PCR product was ligated into the pMal-c2x protein
107 expression plasmid (New England Biolabs) adjacent to the *malE* gene to generate the
108 pMAL-c2x-*malE*-L375-his₁₀ plasmid encoding maltose binding protein (MBP) fusion
109 protein MBP-L375-HIS₁₀. A targeted mutation in the Nudix motif was introduced
110 through use of the QuikChange site-directed mutagenesis kit (Agilent Technologies) to
111 produce a plasmid encoding L375 (E258Q).

112

113 **Synthesis and purification of recombinant L375 protein**

114 Wild-type or mutated pMAL-c2x-*malE*-L375-his₁₀ plasmids were transformed
115 into *Escherichia coli* strain BL21 (EMD Millipore) for subsequent growth in LB broth
116 supplemented with 50 µg/ml carbenicillin and 0.2% (w/v) glucose. MBP-L375-HIS₁₀
117 expression was induced with 0.15 mM isopropyl β-D-1 thiogalactopyranoside (IPTG)
118 followed by growth at 28 °C. After 4 h of induction, cell lysates were produced using
119 sonication. The recombinant protein was sequentially purified using an amylose column
120 (New England Biolabs) followed by a nickel-nitrilotriacetic acid column (Qiagen) and
121 then dialyzed against buffer comprised of 10 mM Tris-HCl pH 7.5, 100 mM NaCl, 10%
122 glycerol, 1 mM DTT, and 2 mM Mg acetate [27]. Recombinant VACV MBP-D10 was
123 produced and purified by affinity column chromatography as detailed in Parrish et al.
124 [13].

125

126 **Synthesis of RNA substrate**

127 The MEGAscript kit (Life Technologies) and pTRI-β-actin-human template
128 (Life Technologies) were used to *in vitro* transcribe a 309-nt actin RNA transcript that
129 was subsequently cap-labeled using recombinant VACV guanylyltransferase/guanine-7-
130 methyltransferase (Epicentre Biotechnologies) in conjunction with capping buffer (50
131 mM Tris-HCl pH 8.0, 6 mM KCl, 1.25 mM DTT, 1.25 MgCl₂), 0.132 µM [α³²P] GTP,
132 and 0.1 mM *S*-adenosylmethionine [28]. The cap-labeled RNA was then purified from
133 unincorporated nucleotides by using a ProbeQuant G-50 gel filtration column (GE
134 Healthcare).

135

136 **RNA decapping assays**

137 0.02 pmol of cap-labeled RNA was incubated with purified recombinant wild-
138 type or mutant MBP-L375-HIS₁₀ in the presence of decapping buffer (100 mM K acetate,
139 10 mM Tris-HCl pH 7.5, 2 mM MgCl₂, 0.5 mM MnCl₂, and 2 mM DTT) in a total
140 volume of 15 µl for 30 min at 37 °C [27]. 2 µl aliquots of each reaction were resolved on
141 a polyethyleneimine-cellulose thin layer chromatography plate (Sigma-Aldrich)
142 developed in 0.75 M LiCl. UV shadowing was used to detect unlabeled nucleotide
143 standards while autoradiography and PhosphorImager analysis (Molecular Dynamics)
144 were used to visualize radioactive signals.

145

146 **Results**

147 **Recombinant Mimivirus L375 exhibits mRNA decapping**

148 **activity**

149 The observation that Mimivirus L375 harbors a Nudix motif, in conjunction with
150 the sequence similarity observed between L375 and ASFV-DP, suggested that L375
151 could possess intrinsic mRNA decapping activity to modulate mRNA turnover during
152 infection. To evaluate if recombinant Mimivirus L375 could decap mRNA, a maltose
153 binding protein (MBP)-L375 fusion protein terminated with C-terminal 10X histidine
154 epitope tag (MBP-L375-HIS₁₀) was synthesized in *Escherichia coli* and purified through
155 successive amylose and nickel-nitrilotriacetic acid columns. Following separation of the
156 purified recombinant protein through sodium dodecyl sulfate-polyacrylamide gel

157 electrophoresis (SDS/PAGE), the expected ~87-kDa band for MBP-L375-HIS₁₀ was
158 observed (Fig 1A).

159

160 **Fig 1. Recombinant Mimivirus L375 hydrolyzes the mRNA cap.** (A) An MBP-L375
161 fusion protein containing a C-terminal 10X histidine epitope tag (MBP-L375-HIS₁₀) was
162 synthesized in *Escherichia coli* and purified by affinity chromatography through
163 successive amylose and nickel-nitrilotriacetic acid columns. The purified MBP-L375-
164 HIS₁₀ protein was separated by SDS/PAGE and visualized by Coomassie blue staining.
165 The locations of the protein mass standards (in kDa) are labeled on the left side of the gel
166 and the ~87 kDa MBP-L375-HIS₁₀ protein is denoted on the right. (B) MBP-L375-HIS₁₀
167 (80 ng) and 0.02 pmol ³²P-cap-labeled actin RNA were added to decapping buffer and
168 incubated at 37 °C for 30 min. After the incubation, an aliquot of the reaction was treated
169 with 2 U of nucleoside diphosphate kinase (NDPK) in the presence of 1 mM ATP at 37
170 °C for 30 min to convert nucleoside diphosphates into nucleoside triphosphates. The
171 products of the reaction were separated on PEI-cellulose TLC plates in 0.75 M LiCl and
172 the radioactive signals were visualized by autoradiography. Non-radioactive nucleotide
173 standards were run in parallel and detected by UV shadowing, as indicated on the right.

174

175 For the mRNA decapping assays, *in vitro* synthesized 309-nt actin RNA was
176 capped, methylated, and radioactively labeled using recombinant VACV RNA
177 guanylyltransferase/guanine-7-methyltransferase in the presence of [α ³²P] GTP and S-
178 adenosylmethionine [28]. The ³²P-cap-labeled RNA substrate was then combined with
179 MBP-L375-HIS₁₀ and the products of the reactions were separated on polyethyleneimine

180 (PEI)-cellulose thin layer chromatography (TLC) plates. Radioactive signals were
181 visualized using either autoradiography or PhosphorImager analysis, whereas unlabeled
182 TLC nucleotide standards were detected by UV shadowing.

183 As expected, in the absence of recombinant L375, the large ^{32}P -cap-labeled RNA
184 stayed at the origin of the TLC plate and no major reaction products were detected; the
185 minor faint spot detected may correspond to unincorporated GTP remaining after
186 purification of the cap-labeled RNA (Fig 1B). When recombinant MBP-L375-HIS₁₀ was
187 included in the reaction, a product was released that migrated the same distance as the
188 unlabeled m⁷GDP standard, demonstrating that L375 cleaves the methylated mRNA cap
189 (Fig 1B). After cap hydrolysis, a residual amount of uncleaved cap-labeled RNA was
190 observed at the origin. Since L375 specifically cleaves methylated-capped structures (see
191 below) and methylation by *S*-adenosylmethionine of the cap-labeled RNA is generally
192 incomplete, some intact, unmethylated cap-labeled RNA is expected to remain at the
193 origin.

194 To confirm that the product released was m⁷GDP, the decapping products were
195 incubated with nucleoside diphosphate kinase (NDPK), an enzyme that phosphorylates
196 nucleoside diphosphates to yield nucleoside triphosphates. After the addition of NDPK,
197 the m⁷GDP product generated by MBP-L375-HIS₁₀ shifted in a downward direction to
198 co-migrate with the m⁷GTP standard (Fig 1B).

199

200 **Recombinant Mimivirus L375 mRNA decapping activity is**
201 **dependent on the Nudix motif**

202 The highly conserved Nudix box consists of the signature sequence
203 GX₅EX₅[UA]XREX₂EEXGU (where U indicates either isoleucine, leucine, or valine and
204 X denotes any amino acid), of which the EX₂EE sequence has been shown to be required
205 for divalent cation binding and catalytic activity [10, 29, 30]. To determine whether the
206 Nudix motif was essential for cap cleavage, a point mutation was created in the essential
207 EX₂EE active site residues of L375. A mutated version of L375 was synthesized in which
208 the glutamic acid at position 258 was changed to glutamine [L375(E258Q)]. The mutated
209 L375(E258Q) protein was expressed in *Escherichia coli* and then purified by affinity
210 chromatography concurrently with the wild-type recombinant proteins. As previously
211 shown, incubation of wild-type recombinant L375 with the capped mRNA substrate
212 resulted in the hydrolysis of the 5' cap and release of m⁷GDP (Fig 2). However, when an
213 equal amount of the mutant L375(E258Q) protein was added to the capped RNA
214 substrate, m⁷GDP was not liberated, confirming that the Nudix motif was essential for
215 cap cleavage and that the recombinant protein was directly responsible for the decapping
216 activity observed in the assay (Fig 2).

217

218 **Fig 2. The mRNA decapping activity of recombinant L375 is dependent on an intact**
219 **Nudix hydrolase motif.** The Nudix motif of MBP-L375-HIS₁₀ was subjected to site-
220 directed mutagenesis to convert the glutamic acid residue at position 258 into a glutamine
221 residue, thereby producing L375(E258Q). The mutant and wild-type proteins were
222 expressed and purified in parallel as described in Fig 1A and equivalent amounts of the
223 two proteins (50 ng) were added to separate mRNA decapping assays conducted as in Fig
224 1B.

225

226 **Recombinant Mimivirus L375 specifically cleaves methylated** 227 **cap structures**

228 Since Nudix enzymes can cleave a broad range of substrates, it was important to
229 investigate the specificity of L375 for the 5' m⁷GpppN mRNA cap [31]. The mRNA cap
230 contains a unique methyl group at position 7 on the guanine base, a structural feature
231 often recognized by proteins that exclusively bind and/or cleave the mRNA cap. To
232 examine the selectivity of L375 for the 5' m⁷GpppN cap structure, an unmethylated
233 GpppN-capped RNA was synthesized by excluding the *S*-adenosylmethionine methyl
234 donor from the capping reaction, and the unmethylated substrate was subsequently
235 incubated with recombinant L375. Importantly, recombinant L375 was not able to
236 significantly cleave the unmethylated GpppN cap to release GDP, indicating that this
237 enzyme specifically recognizes the methylated mRNA cap (Fig 3). As expected, when
238 equivalent amounts of mutant L375(E258Q) protein was added to the unmethylated cap-
239 labeled substrate, no products were generated.

240

241 **Fig 3. Recombinant L375 specifically cleaves methylated cap structures.** (A) The
242 ³²P-cap-labeled actin 309-nt RNA substrate was synthesized either in the presence
243 (+CH₃) or absence (-CH₃) of the methyl donor *S*-adenosylmethionine. 0.02 pmol of
244 methylated or unmethylated RNA substrate was incubated with either 50 ng of
245 recombinant wild-type L375 or mutant L375 (E258Q) in mRNA decapping assays as
246 described in Fig 1B.

247

248 **Mimivirus L375 mRNA decapping activity increases with time**
249 **and enzyme concentration**

250 A time course experiment revealed that the amount of m⁷GDP product released by
251 L375 increased through time, as expected for an enzyme (Fig 4A). Likewise, increasing
252 amounts of L375 enzyme resulted in the release of more m⁷GDP product, until saturation
253 was reached (Fig 4B). As noted for above and similar to other viral mRNA decapping
254 enzymes, a proportion of the substrate remains resistant to cleavage despite high enzyme
255 concentrations (~28%), because some of the ³²P-cap-labeled RNA remains unmethylated
256 and therefore not a viable substrate. This observation, along with the finding that the
257 presence of uncapped RNA inhibits L375 mRNA decapping activity (see Fig 5 below),
258 hindered our ability to determine the kinetic coefficients of the reaction.

259

260 **Fig 4. Recombinant L375 mRNA decapping activity increases with time and**
261 **enzyme concentration.** (A) 60 ng of recombinant L375 was incubated with 0.02 pmol
262 ³²P-cap-labeled actin RNA substrate in decapping buffer at 37 °C for the time indicated
263 on the graph. After separation of the reaction products on PEI-cellulose TLC plates, the
264 percentage of m⁷GDP released was calculated by PhosphorImager analysis. (B) The
265 indicated amount of recombinant L375 was added to 0.02 pmol ³²P-cap-labeled actin
266 RNA substrate for mRNA decapping assays performed as in Fig 1B. The percentage of
267 m⁷GDP liberated was quantified using a PhosporImager.

268

269 **Uncapped RNA inhibits Mimivirus L375 mRNA decapping**

270 **activity**

271 The viral mRNA decapping enzymes characterized to date have all been shown to
272 be inhibited by the addition of uncapped RNA, suggesting that these enzymes recognize
273 and bind the RNA moiety during substrate identification [13-15]. To evaluate if
274 Mimivirus L375 also interacts with the RNA body during substrate recognition,
275 increasing molar amounts of uncapped RNA were added to the reaction and the
276 percentage of m⁷GDP product released was calculated. Addition of uncapped RNA
277 competitor significantly decreased L375 decapping activity, in a manner almost identical
278 to that observed for VACV D10 (Fig 5). For example, a 20-fold molar excess of
279 competitor RNA reduced both L375 and VACV decapping activity by 62%, suggesting
280 that L375 binds the RNA body during substrate recognition (Fig 5).

281

282 **Fig 5. Recombinant L375 mRNA decapping activity is reduced by the addition of**

283 **uncapped RNA competitor.** 80 ng of recombinant L375 or VACV D10 and 0.02 pmol

284 ³²P-cap-labeled 309-nt actin RNA were incubated with increasing amounts of uncapped,

285 non-radioactive 309-nt actin RNA in mRNA decapping assays conducted as described in

286 Fig 1B. The percentage of m⁷GDP product released was determined by using a

287 PhosphorImager.

288

289 **Methylated nucleotides inhibit L375 mRNA decapping activity**

290 It was previously shown that the decapping activity of VACV D9 and D10 was
291 inhibited by m⁷GTP, m⁷GDP, and m⁷GpppG, structures that mimic the mRNA cap and
292 therefore may compete for binding [13, 14]. Conversely, ASFV-DP was not inhibited by
293 any of the three methylated cap analogs, indicating that ASFV-DP may exclusively use
294 the RNA moiety to locate its substrate [15]. To evaluate the effect of methylated
295 nucleotides on L375 substrate cleavage, increasing quantities of m⁷GTP, m⁷GDP, and
296 m⁷GpppG or unmethylated alternatives of these nucleotides were included in the
297 reactions and the amount of product generated was calculated. Interestingly, the most
298 robust inhibition of L375 decapping activity was observed for m⁷GTP, mirroring the
299 results seen for VACV D10 (Figs 6A, 6B, and 6C). m⁷GDP also inhibited L375 cap
300 cleavage, but the effect was more modest than that observed for m⁷GTP (Fig 6B).
301 Surprisingly, m⁷GpppG did not significantly reduce the ability of L375 to decap mRNA,
302 in contrast to the observed reduction of D10 decapping activity by this cap analog (Fig
303 6C). In support of the specificity of L375 for the methylated cap, the unmethylated
304 versions of the three nucleotides (GDP, GTP, and GpppG) did not significantly inhibit
305 L375 decapping activity. These results suggest that L375 may recognize both the
306 methylated cap structure and the RNA moiety during substrate identification.

307

308 **Fig 6. Recombinant L375 mRNA decapping activity is inhibited by addition of**
309 **m⁷GTP or m⁷GDP.** (A) 80 ng of recombinant L375 or VACV D10 and 0.02 pmol ³²P-
310 cap-labeled actin RNA were incubated together in the presence of increasing quantities of
311 m⁷GTP or GTP in mRNA decapping assays as described in Fig 1B. The percentage of
312 m⁷GDP liberated was calculated through PhosphorImager analysis. (B) mRNA decapping

313 assays were performed as in Panel A with increasing amounts of m⁷GDP or GDP. (C)
314 mRNA decapping assays were performed as described in Panel A with increasing
315 amounts of m⁷GpppG cap analog or GpppG.

316

317 **Discussion**

318 Nudix hydrolases cleave a broad range of substrates, a subset of which cleave the
319 5' mRNA cap. The importance of these enzymes is illustrated by their conservation
320 between the living organisms (prokaryotes and eukaryotes), as well as their presence in
321 some of the non-living viruses. Three NCLDV Nudix hydrolases have been characterized
322 to date, VACV D9, VACV D10, and ASFV-DP. Each of these enzymes have been shown
323 to possess intrinsic mRNA decapping activity *in vitro* [13-15]. Importantly, ASFV-DP
324 shares sequence similarity to both the well-characterized eukaryotic Dcp2 Nudix mRNA
325 decapping enzyme and Mimivirus L375, the focus of this work [12, 21-26].

326 Here we show that the Mimivirus Nudix enzyme L375 hydrolyzed the mRNA cap
327 to release m⁷GDP; a reaction that is dependent on an intact Nudix box. Like L375,
328 VACV D9 was shown to preferentially hydrolyze methylated rather than unmethylated
329 mRNA caps [14]. In contrast, ASFV-DP has a broader nucleotide substrate range that
330 includes GTP [15, 20]. Eukaryotic Dcp2 has been reported to preferentially cleave
331 methylated rather than unmethylated cap structures, although some decapping activity
332 has been detected with unmethylated mRNA cap substrates depending on the divalent
333 cation present in the reaction buffer [23-25, 27, 32].

334 Similar to the viral and eukaryotic mRNA decapping enzymes characterized to
335 date, uncapped competitor RNA reduced L375 decapping activity, suggesting that L375
336 also uses the RNA moiety for substrate selection [13-15, 25, 27, 33]. Previous studies
337 showed that uncapped competitor RNA more potently inhibited the mRNA decapping
338 activity of ASFV-DP compared to VACV D9 or D10 (ASFV-DP>D9>D10), indicating
339 that ASFV-DP may have a higher affinity for RNA than the poxvirus enzymes [13-15].
340 In this work, the inhibition of L375 by competitor RNA more closely resembled that of
341 VACV D10, suggesting that L375 may have a lower affinity for RNA than ASFV-DP,
342 despite their greater sequence similarity.

343 The strong affinity of ASFV-DP for RNA was confirmed through an
344 electrophoretic mobility shift assay, in which the migration of uncapped RNA was
345 impeded with the addition of ASFV-DP [15]. Subsequent *in vivo* experiments confirmed
346 that ASFV interacts with viral and host mRNAs during infection, a property dependent
347 on the N-terminus of the protein, rather than the Nudix motif [21]. ASFV-DP also
348 exhibited different levels of binding efficiency depending on the specific mRNA, similar
349 to Dcp2 [21]. For example, yeast Dcp2 preferentially binds capped mRNAs with a stem-
350 loop structure within the first 10 bases of the sequence. [34, 35].

351 As observed for VACV D9 and D10 (but not for ASFV-DP), addition of
352 methylated cap derivatives reduced L375 decapping activity, suggesting that L375
353 recognizes the cap structure in addition to the RNA body [13, 14]. Specifically, L375
354 decapping activity was most potently inhibited by m⁷GTP, followed by m⁷GDP, whereas
355 the effect of m⁷GpppG was negligible (m⁷GTP>m⁷GDP>m⁷GpppG). In comparison, the
356 decapping activity of both VACV D9 and D10 was diminished by all three methylated

357 cap derivatives, with the most striking reduction also observed with m⁷GTP [13, 14].
358 Interestingly, VACV D10 was more sensitive to inhibition by methylated nucleotides
359 than either L375 or VACV D9, suggesting a greater importance of the cap structure for
360 substrate recognition for this enzyme [13, 14].

361 In contrast, ASFV-DP was not inhibited by addition of methylated cap
362 derivatives, nor could it cleave free methylated cap analog *in vitro*, suggesting that for
363 ASFV-DP, the RNA body is critical during substrate identification [15, 20]. Like ASFV-
364 DP, the mRNA decapping activity of most eukaryotic Dcp2 enzymes is not affected by
365 the addition of methylated cap analogs, suggesting these enzymes primarily recognize the
366 RNA moiety to locate target substrates [23-25, 27]. Hence, the inhibition of L375
367 decapping activity by methylated cap derivatives more closely resembles VACV D9 and
368 D10 rather than that of ASFV-DP or Dcp2.

369 The purpose of mRNA decapping during viral infection has been revealed
370 through *in vivo* studies characterizing VACV D9, D10, and ASFV-DP. Increased
371 expression of VACV D9, VACV D10, or ASFV-DP resulted in enhanced mRNA
372 turnover of capped viral and host transcripts, further validating that these enzymes decap
373 mRNA to elicit subsequent mRNA degradation [17, 21]. Interestingly, over-expression of
374 ASFV-DP increased degradation of some mRNA transcripts more than others, suggesting
375 that the degree of mRNA turnover induced by ASFV-DP could be selective, as has been
376 shown for Dcp2 [21, 34, 35].

377 In complementary genetic studies in VACV, deletion or inactivation of D10
378 resulted in persistence of viral and host mRNAs, a delay in the shutoff of host protein
379 synthesis, and a modest reduction of virulence in animal hosts, whereas deletion of D9

380 did not produce any noticeable defects [17-19, 36]. When both D9 and D10 were
381 inactivated concurrently, viral replication was severely impaired both *in vitro* and *in vivo*,
382 suggesting that these two enzymes work together synergistically [37]. The substantial
383 replication defects exhibited by the double D9/D10 mutant virus were shown to result
384 from the accumulation of excess amounts of viral double-stranded RNA (dsRNA) that
385 subsequently activated the host's innate immune defenses to curtail infection [37]. These
386 results suggest that in addition to modulating viral and cellular mRNA turnover, D9 and
387 D10 also induce viral dsRNA degradation to avoid activating host anti-viral responses.
388 Furthermore, cellular RNA exonuclease Xrn1, which degrades RNA following
389 decapping, was also required to avoid aberrant viral dsRNA accumulation, suggesting the
390 viral mRNA decapping enzymes work in concert with cellular Xrn1 to degrade viral
391 dsRNA to evade the host immune system [38].

392 Like VACV and ASFV, Mimivirus encodes its own mRNA capping enzyme and
393 directs a sequential cascade of viral gene expression consisting of early, intermediate, and
394 late phases; therefore, decapping of viral mRNAs by L375 could provide a mechanism to
395 orchestrate the transitions between viral gene expression during infection [2, 39].
396 Furthermore, mRNA decapping by L375 during Mimivirus infection could be responsible
397 for the degradation of host mRNAs to elicit the shutdown of host protein synthesis,
398 allowing viral transcripts preferential access to the host translation machinery [2].

399 In contrast to the animal hosts of VACV and ASFV, Mimivirus primarily infects
400 unicellular *Acanthamoeba* species, and therefore does not require L375 mRNA
401 decapping activity to evade the complex vertebrate immune systems. However,
402 Mimivirus could still use selective mRNA decapping and degradation of specific host

403 mRNAs to promote a robust *Acanthamoeba* infection. Future *in vivo* studies will help
404 elucidate the role of L375 mRNA decapping and decay during Mimivirus infection.

405

406 **Acknowledgments**

407 We sincerely thank Bernard Moss for his generous support of this work, guidance,
408 and helpful suggestions. In addition, we are grateful to Wolfgang Resch, P.S.

409 Satheshkumar, Zhilong Yang, and Cheng Huang for helpful discussions and technical
410 assistance.

411

412 **References**

413 1. Raoult D, Audic S, Robert C, Abergel, C, Renesto, P, Ogata H, et al. The 1.2-megabase
414 genome sequence of Mimivirus. *Science*. 2004; 304(5700):1344-1350.

415 2. Legendre M, Audic S, Poirot O, Hingamp P, Seltzer V, Byrne D, et al. mRNA deep
416 sequencing reveals 75 new genes and a complex transcriptional landscape in Mimivirus.
417 *Genome Res*. 2010; 20(5):664-674.

418 3. Legendre M, Santini S, Rico A, Claverie J. Breaking the 1000-gene barrier for Mimivirus
419 using ultra-deep genomic and transcriptome sequencing. *Virology*. 2011 March 4. doi:
420 [10.1186/1743-422X-8-99](https://doi.org/10.1186/1743-422X-8-99).

421 4. Iyer LM, Aravind L, Koonin EV. Common origin of four diverse families of large eukaryotic
422 DNA viruses. *J. Virol*. 2001; 75(23):11720-11734.

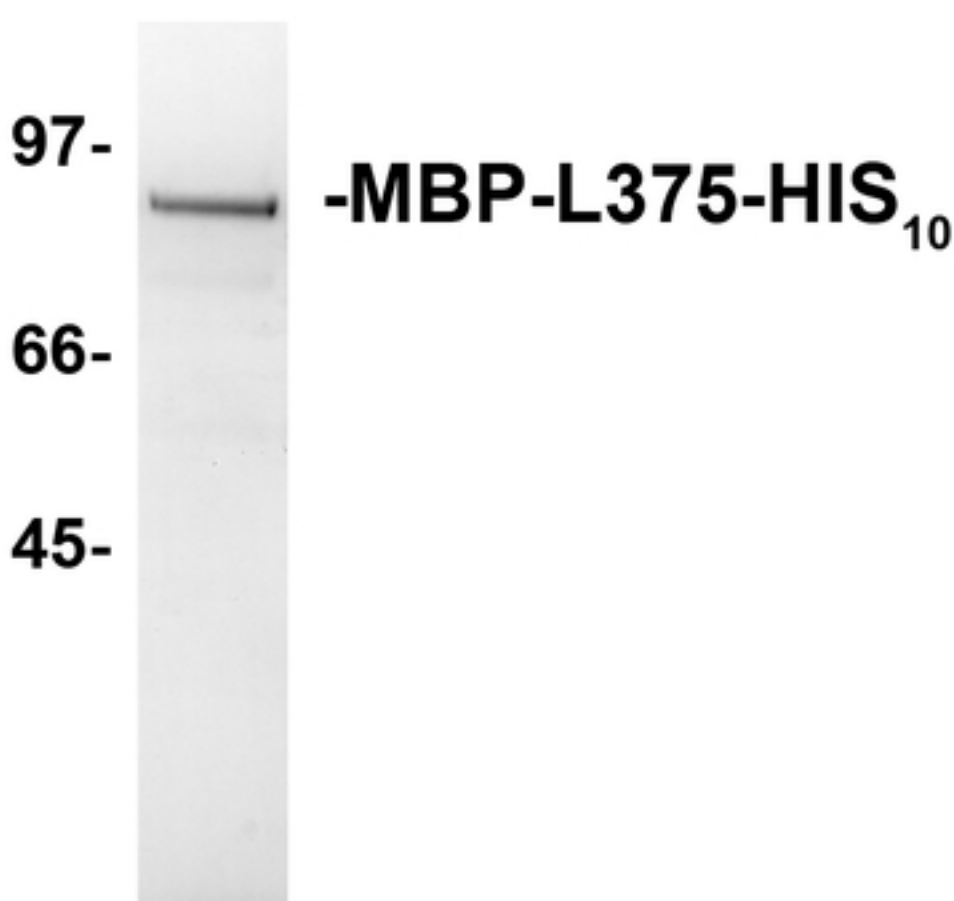
423 5. Iyer LM, Balaji S, Koonin EV, Aravind L. Evolutionary genomics of nucleocytoplasmic
424 large DNA viruses. *Virus Res*. 2006; 117(1):156-184.

- 425 6. Yutin N, Wolf YI, Raoult D, Koonin EV. Eukaryotic large nucleo-cytoplasmic DNA
426 viruses: Clusters of orthologous genes and reconstruction of viral genome evolution.
427 *Virol. J.* 2009; 6(223). doi: [10.1186/1743-422X-6-223](https://doi.org/10.1186/1743-422X-6-223).
- 428 7. Yutin N, Koonin EV. Hidden evolutionary complexity of nucleo-cytoplasmic large
429 DNA viruses of eukaryotes. *Virol. J.* 2012; 9(161) doi: [https://doi.org/10.1186/1743-](https://doi.org/10.1186/1743-422X-9-161)
430 [422X-9-161](https://doi.org/10.1186/1743-422X-9-161).
- 431 8. Colson P, Pagnier I, Yoosuf N, Fournous G, La Scola B, Raoult D. “Marseilleviridae”, a new
432 family of giant viruses infecting amoebae. *Arch. Virol.* 2013; 158(4):915-920.
- 433 9. Koonin EV, Yutin N. Multiple evolutionary origins of giant viruses. *F1000Res.* 2018
434 Nov. 22. doi: [10.12688/f1000research.16248.1](https://doi.org/10.12688/f1000research.16248.1)
- 435 10. Bessman MJ, Frick DN, O'Handley SF. The MutT proteins or "Nudix" hydrolases, a family
436 of versatile, widely distributed, "housecleaning" enzymes. *J. Biol. Chem.* 1996;
437 271(41):25059-25062.
- 438 11. McLennan AG. The Nudix hydrolase superfamily. *Cell Mol. Life Sci.* 2006; 63:123-143.
- 439 12. McLennan, AG. Decapitation: Poxvirus makes RNA lose its head. *Trends Biochem. Sci.*
440 2007; 32(7):297-299.
- 441 13. Parrish S, Resch W, Moss B. Vaccinia virus D10 protein has mRNA decapping activity,
442 providing a mechanism for control of host and viral gene expression. *Proc. Natl. Acad. Sci.*
443 *U. S. A.* 2007; 104(7):2139-2144.
- 444 14. Parrish S, Moss B. Characterization of a second vaccinia virus mRNA-decapping enzyme
445 conserved in poxviruses. *J. Virol.* 2007; 81(23):12973-12978.
- 446 15. Parrish S, Hurchalla M, Liu SW, Moss B. The African swine fever virus g5R protein
447 possesses mRNA decapping activity. *Virology.* 2009; 393(1):177-182.

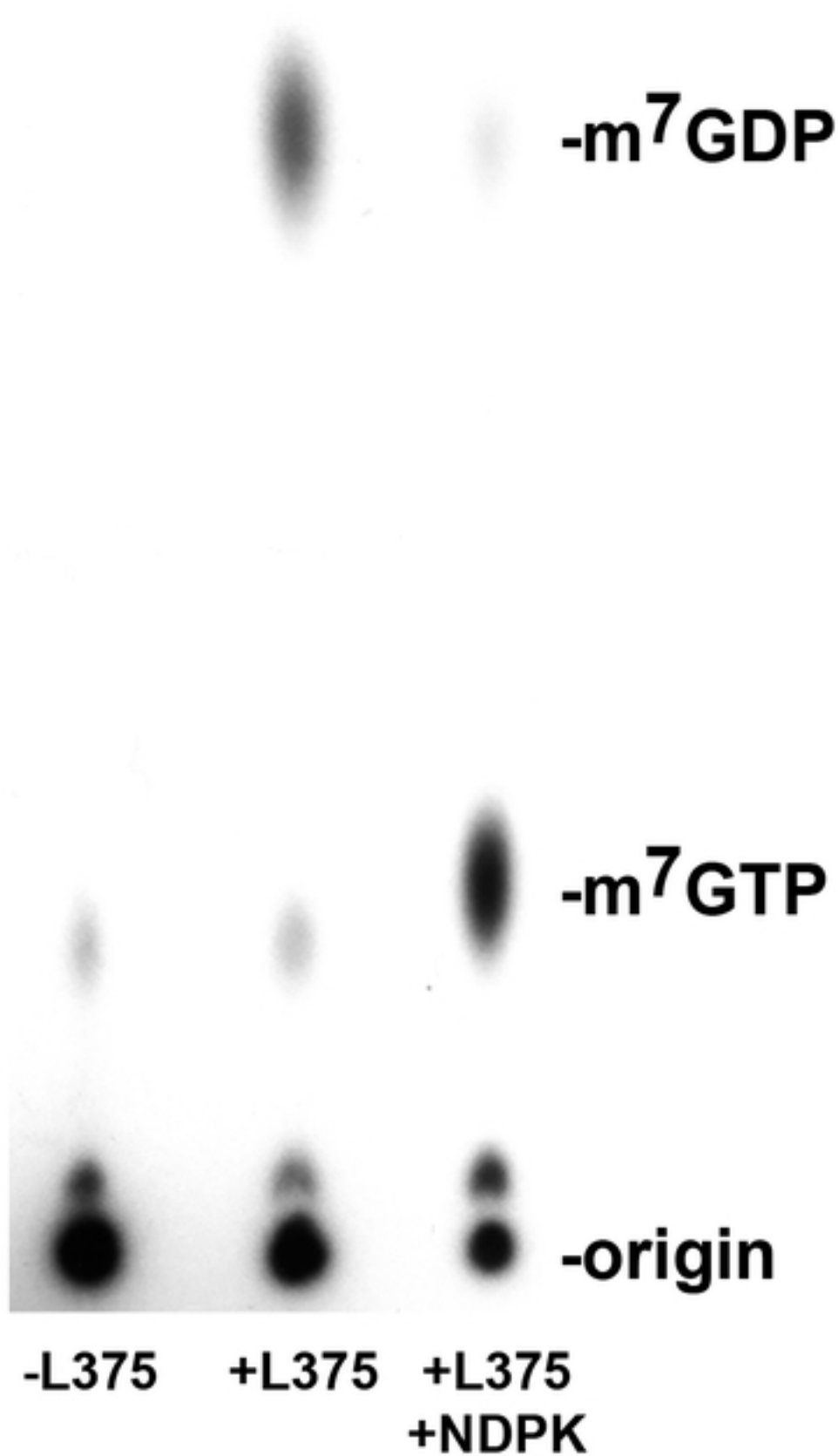
- 448 16. Lee-Chen GJ, Niles EG. Transcription and translation mapping of the 13 genes in the
449 vaccinia virus HindIII D fragment. *Virology*. 1988; 163(1):52-63.
- 450 17. Shors T, Keck JG, Moss B. Down regulation of gene expression by the vaccinia virus D10
451 protein. *J. Virol.* 1999; 73(1):791-796.
- 452 18. Parrish S, Moss B. Characterization of a vaccinia virus mutant with a deletion of the D10R
453 gene encoding a putative negative regulator of gene expression. *J. Virol.* 2006; 80(2):553-
454 561.
- 455 19. Dvoracek B, Shors T. Construction of a novel set of transfer vectors to study vaccinia virus
456 replication and foreign gene foreign gene expression. *Plasmid*. 2003; 49(1):9-17.
- 457 20. Cartwright JL, Safrany ST, Dixon LK, Darzynkiewicz E, Stepinski J, Burke R, McLennan,
458 AG. The g5R (D250) gene of African swine fever virus encodes a Nudix hydrolase that
459 preferentially degrades diphosphoinositol polyphosphates. *J. Virol.* 2002; 76(3):1415-1421.
- 460 21. Quintas A, Pérez-Núñez D, Sánchez E, Nogal M, Hentze M, Castelló A, Revilla Y.
461 Characterization of the African Swine Fever Virus decapping enzyme during
462 infection. *J. Virol.* 2017; 91(24):e00990-17. doi: 10.1128/JVI.00990-17.
- 463 22. Dunckley T, Parker R, The DCP2 protein is required for mRNA decapping in
464 *Saccharomyces cerevisiae* and contains a functional MutT motif. *EMBO J.* 1999; 18(19),
465 5411-5422.
- 466 23. Wang Z, Jiao X, Carr-Schmid A, Kiledjian M. The hDcp2 protein is a mammalian mRNA
467 decapping enzyme. *Proc. Natl. Acad. Sci. U. S. A.* 2002; 99(20):12663-12668.
- 468 24. van Dijk E, Cougot N, Meyer S, Babajko S, Wahle E, Seraphin B. Human Dcp2: a
469 catalytically active mRNA decapping enzyme located in specific cytoplasmic structures.
470 *EMBO J.* 2002; 21(24):6915-6924.

- 471 25. Cohen LS, Mikhli C, Jiao X, Kiledjian M, Kunkel G, Davis RE. Dcp2 decaps
472 m^{2,2,7}GpppN-capped RNAs, and its activity is sequence and context dependent. *Mol. Cell*
473 *Biol.* 2005; 25(20): 8779-8791.
- 474 26. Xu J, Yang JY, Niu QW, Chua NH. *Arabidopsis* DCP2, DCP1, and VARICOSE form a
475 decapping complex required for postembryonic development. *Plant Cell.* 2006;
476 18(12):3386-3398.
- 477 27. Piccirillo C, Khanna R, Kiledjian M. Functional characterization of the mammalian mRNA
478 decapping enzyme hDcp2. *RNA.* 2003; 9(90):1138-1147.
- 479 28. Martin SA, Moss B. Modification of RNA by mRNA guanylyltransferase and mRNA
480 (guanine-7-)methyltransferase from vaccinia virions. *J. Biol. Chem.* 1975; 250(24):9330-
481 9335.
- 482 29. Koonin E. A highly conserved sequence motif defining the family of MutT-related proteins
483 from eubacteria, eukaryotes and viruses. *Nucleic Acids Res.* 1993; 21(20):4847.
- 484 30. Mildvan AS, Xia Z, Azurmendi HF, Saraswat V, Legler PM, Massiah MA et al. Structures
485 and mechanisms of Nudix hydrolases. *Arch. Biochem. Biophys.* 2005; 433(1):129-143.
- 486 31. McLennan AG. Substrate ambiguity among the nudix hydrolases: biologically significant,
487 evolutionary remnant, or both? *Cell Mol. Life Sci.* 2013; 70(3):373-385.
- 488 32. Song M, Bail S, Kiledjian M. Multiple Nudix family proteins possess mRNA decapping
489 activity. *RNA.* 2013; 19(3):390-399.
- 490 33. Gunawardana D, Cheng HC, Gayler KR. Identification of functional domains in *Arabidopsis*
491 *thaliana* mRNA decapping enzyme (AtDcp2). *Nucleic Acids Res.* 2008; 36(1):203-216.
- 492 34. Li Y, Song M, Kiledjian M. Transcript-specific decapping and regulated stability by the
493 human Dcp2 decapping protein. *Mol. Cell Biol.* 2008; 28(3):939-948.

- 494 35. Li Y, Ho E, Gunderson S, Kiledjian M. Mutational analysis of a Dcp2-binding element
495 reveals general enhancement of decapping by 5-end stem-loop structures. *Nucleic Acid Res.*
496 2009; 37(7):2227-2237.
- 497 36. Liu SW, Wyatt LS, Orandle MS, Minai M, Moss B. The D10 decapping enzyme of vaccinia
498 virus contributes to decay of cellular and viral mRNAs and to virulence in mice. *J. Virol.*
499 2014; 88(1):202-211.
- 500 37. Liu SW, Katsafanas GC, Liu R, Wyatt LS, Moss B, Poxvirus decapping enzymes enhance
501 virulence by preventing the accumulation of dsRNA and the induction of innate antiviral
502 response. *Cell Host Microbe.* 2015; 17(3):320-331.
- 503 38. Burgess H, Mohr I. Cellular 5'-3' mRNA exonuclease Xrn1 controls double-stranded RNA
504 accumulation and anti-viral responses. *Cell Host Microbe.* 2015; 17(3): 332-344.
- 505 39. Benarroch D, Smith P, Shuman S. Characterization of a trifunctional Mimivirus mRNA
506 capping enzyme and crystal structure of the RNA triphosphate domain. *Structure.* 2008;
507 16(4):501-512.

A

bioRxiv preprint doi: <https://doi.org/10.1101/2021.01.11.426193>; this version posted January 11, 2021 (which was not certified by peer review) is the author/funder, who has granted bioRxiv a license to display the preprint in perpetuity. It is made available under a [CC-BY 4.0 International license](#).

B

Figure

-m⁷GDP

bioRxiv preprint doi: <https://doi.org/10.1101/2021.01.11.426193>; this version posted January 11, 2021. The copyright holder for this preprint (which was not certified by peer review) is the author/funder, who has granted bioRxiv a license to display the preprint in perpetuity. It is made available under aCC-BY 4.0 International license.

-origin

-L375

+L375

**+L375
E258Q**

Figure

-m⁷GDP

bioRxiv preprint doi: <https://doi.org/10.1101/2021.01.11.426193>; this version posted January 11, 2021. The copyright holder for this preprint (which was not certified by peer review) is the author/funder, who has granted bioRxiv a license to display the preprint in perpetuity. It is made available under aCC-BY 4.0 International license.

-GDP

-origin

**+CH₃
-L375**

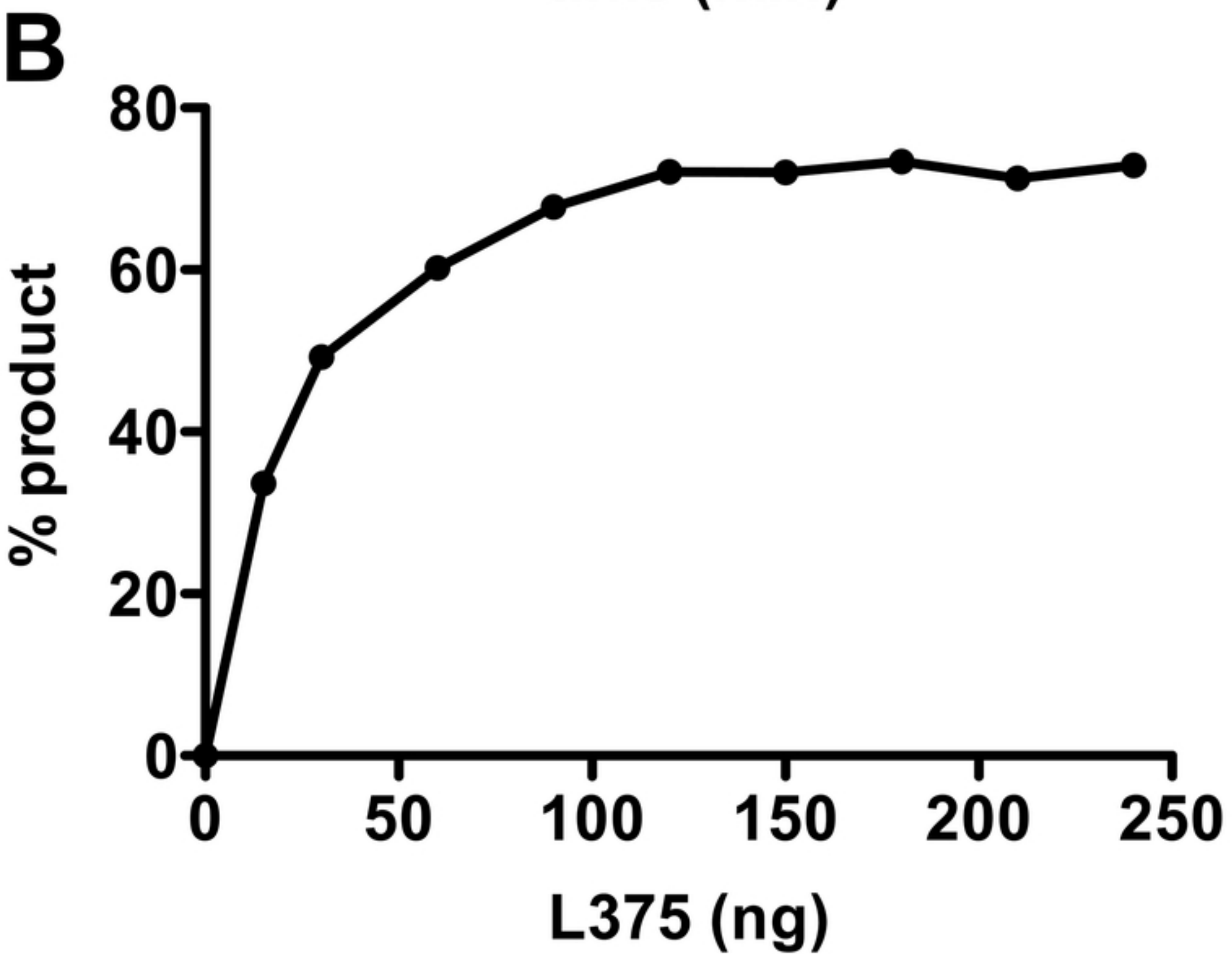
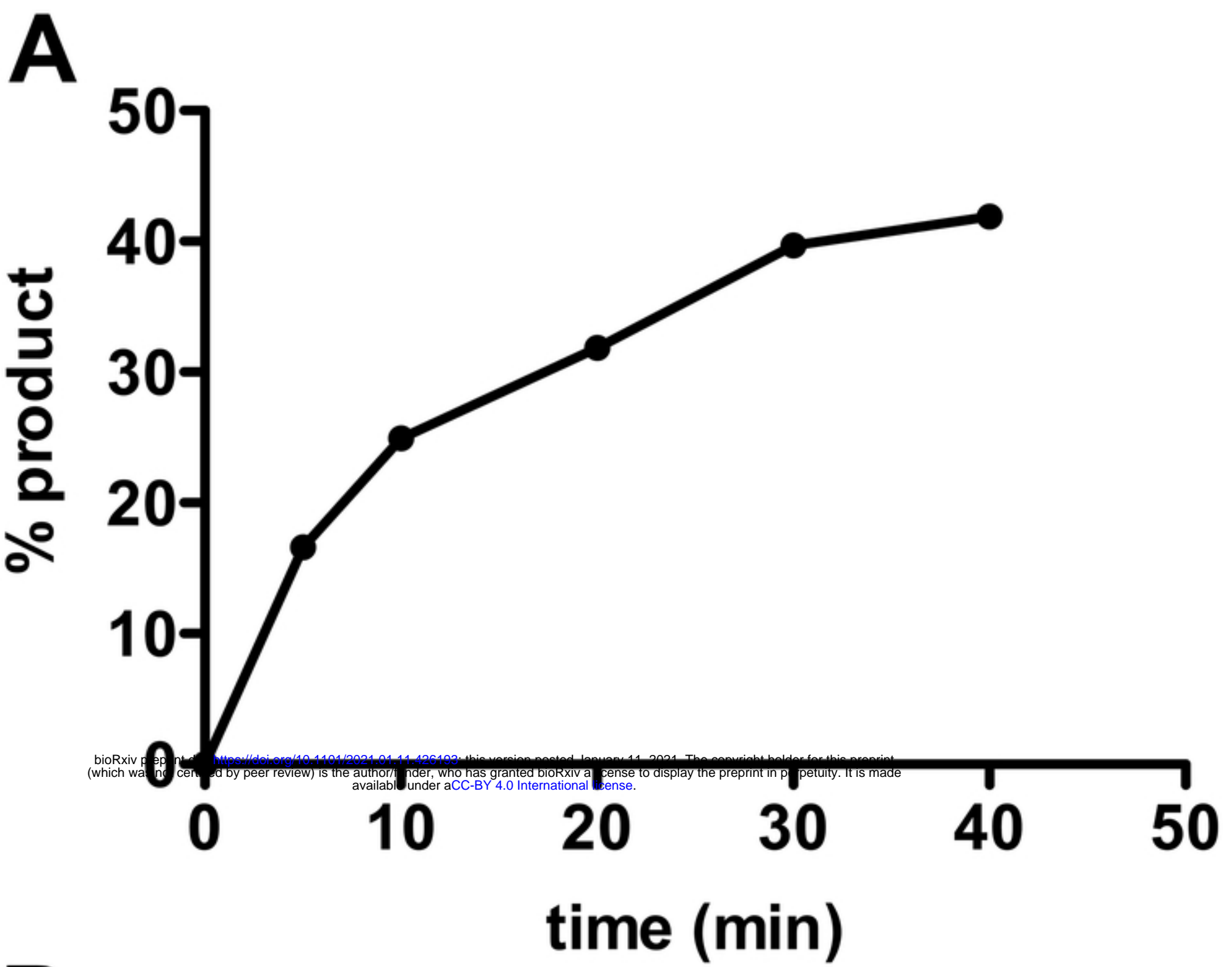
**+CH₃
+L375**

**-CH₃
-L375**

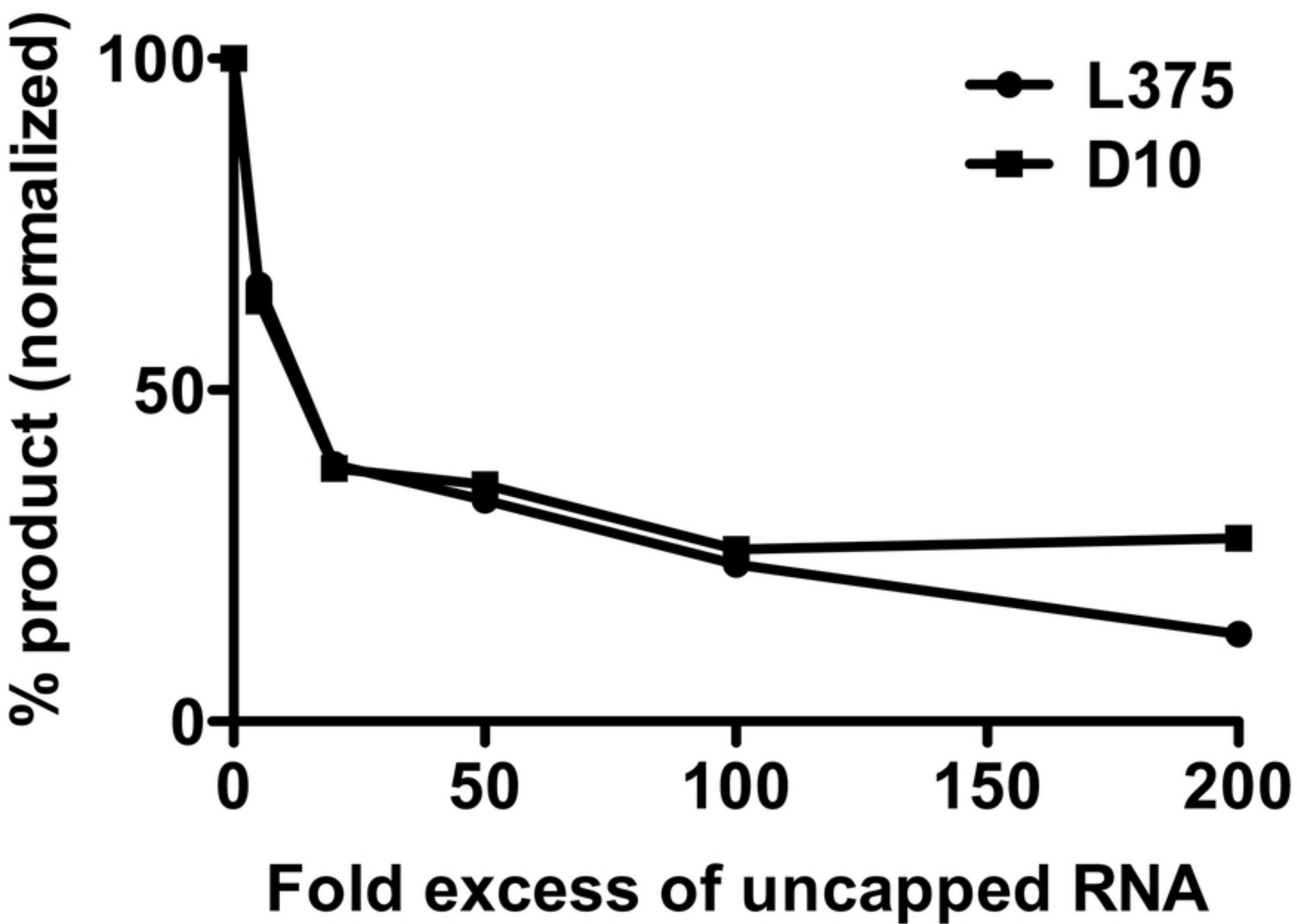
**-CH₃
+L375**

**-CH₃
+L375
E258Q**

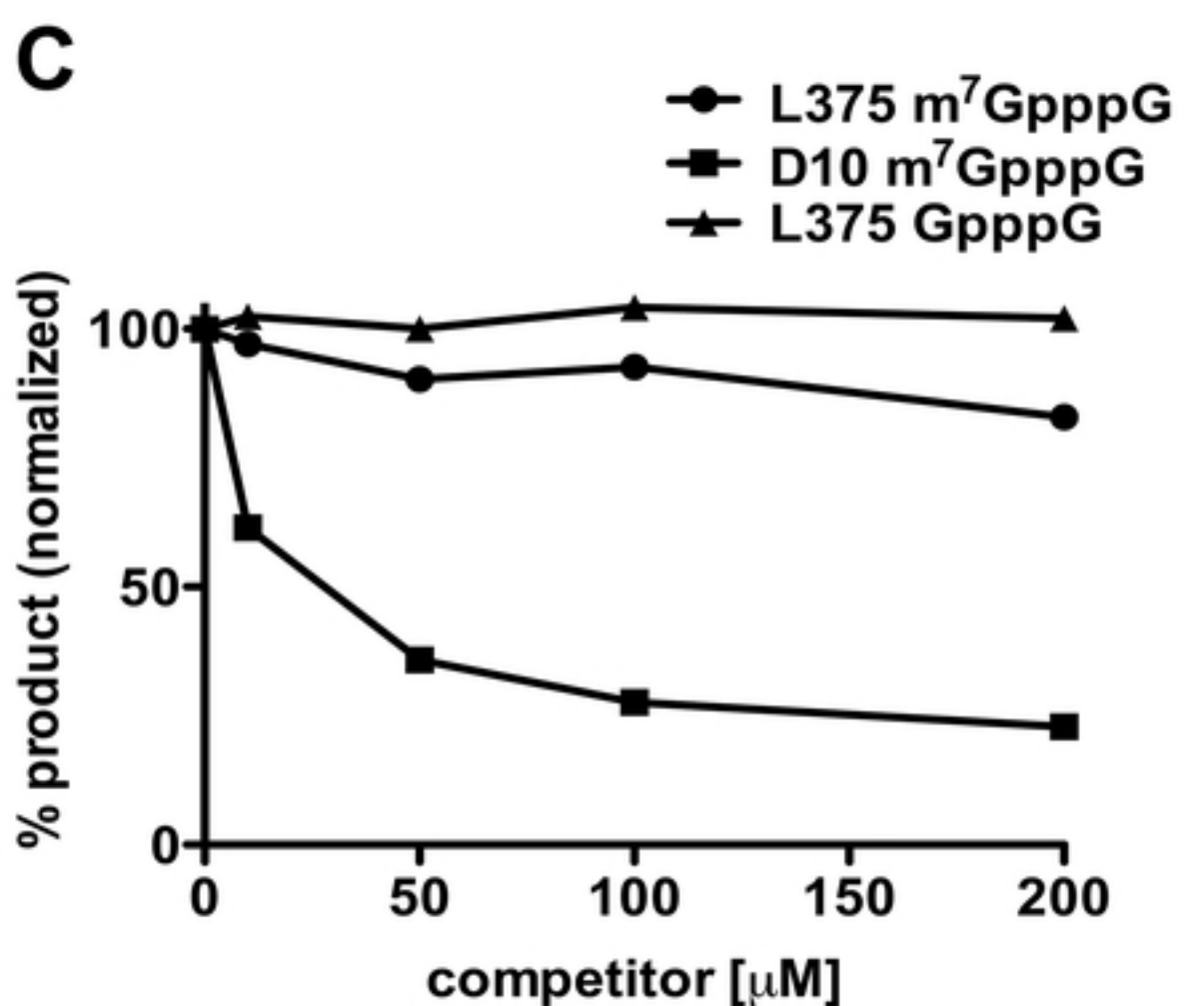
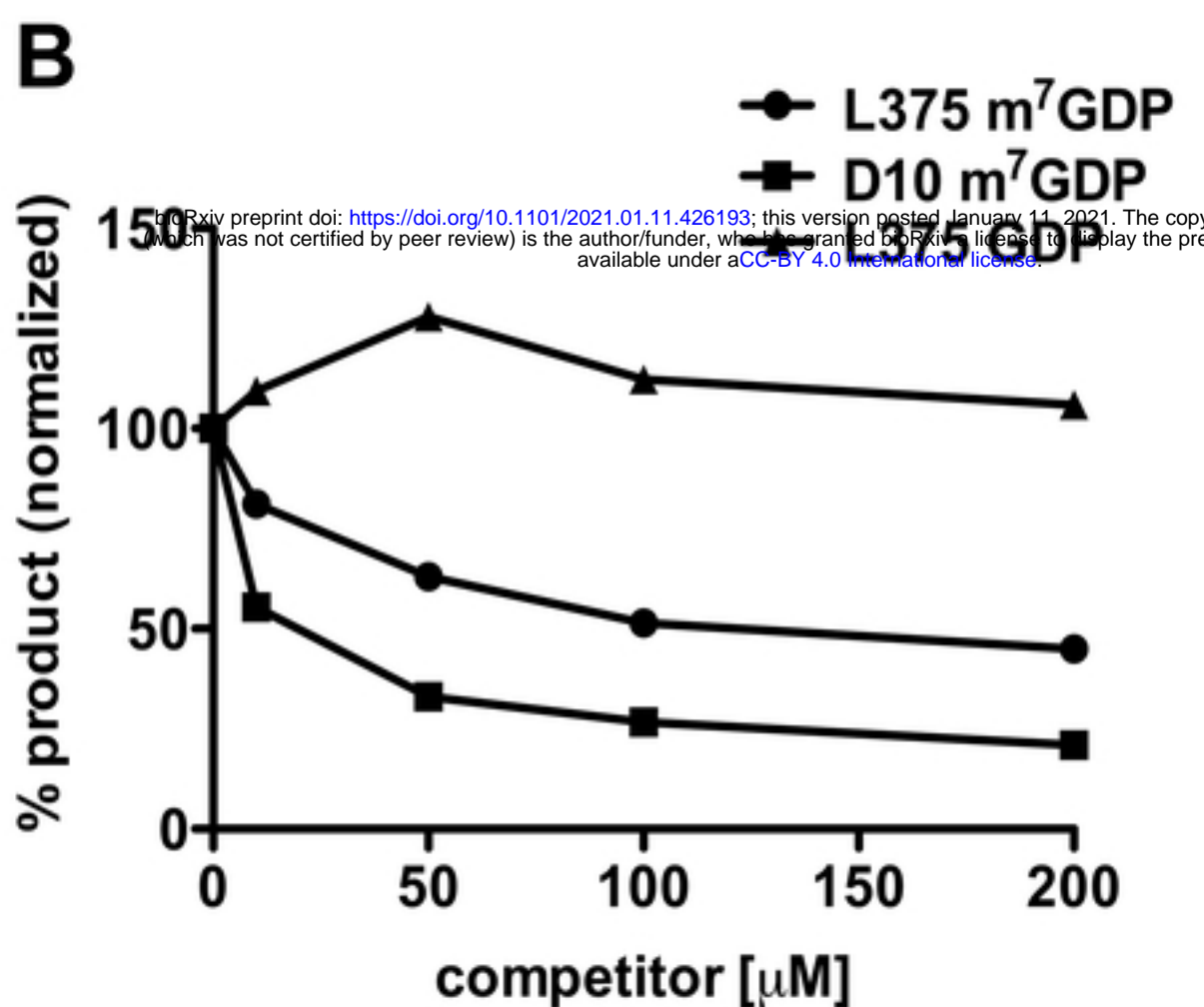
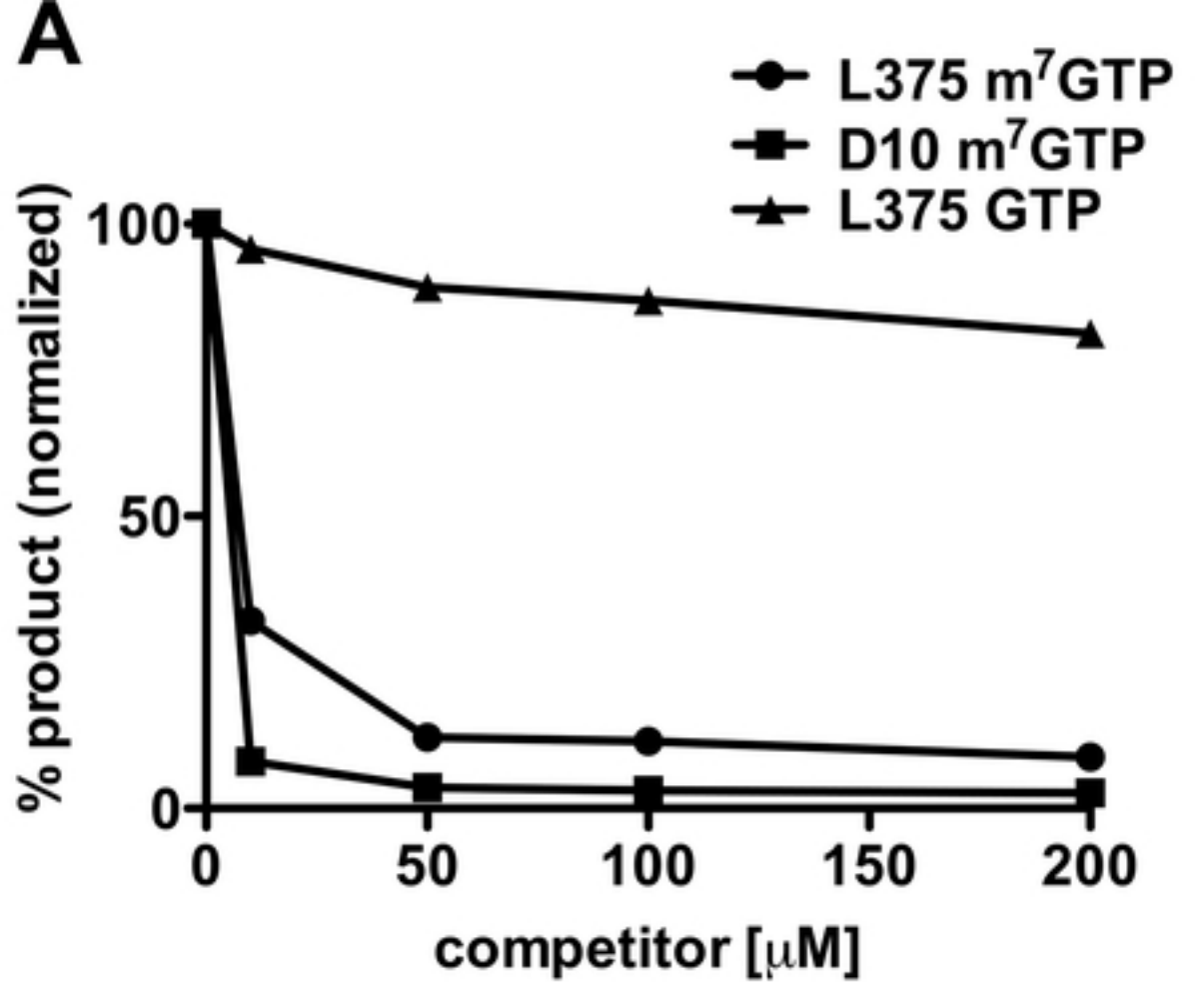
Figure



Figure



Figure



Figure